ACTA NEUROBIOLOGIAE EXPERIMENTALIS

Research paper Acta Neurobiol Exp 2009, 69: 413–428

Immunolocalization of STIM1 in the mouse brain

Anna Skibinska-Kijek[1]*, Marta B. Wisniewska[1], Joanna Gruszczynska-Biegala[1], Axel Methner[3], and Jacek Kuznicki[1,2]

[1] Lab. of Neurodegeneration, International Institute of Molecular and Cell Biology, Warsaw, Poland, *Email: askib@iimcb.gov.pl;
[2] Nencki Institute of Experimental Biology, Polish Academy of Sciences, Warsaw, Poland;
[3] Department of Neurology, Heinrich Heine University, Düsseldorf, Germany

Capacitative Calcium Entry (CCE) in neurons seems to depend, as in non-excitatory cells, on endoplasmic reticulum calcium sensors STIM1 or STIM2. We show localization of STIM1 in the mouse brain by immunohistochemistry with a specific antibody. STIM1 immunoreactivity has wide, but not uniform, distribution throughout the brain and is observed in neuropil and cells. The most intensive immunoreactivity is observed in Purkinje neurons of cerebellum. High/moderate levels of immunostaining are found in hippocampus, cerebral cortex and in cortico-medial amygdala, low in thalamus and basolateral amygdala. Co-staining with anti-NeuN antibody identify STIM1 immunopositive cells as neurons. Real time PCR demonstrates that *Stim2* expression is 7-fold higher than that of *Stim1* in hippocampus and 3-fold in other regions. Immunoblotting confirms that levels of STIMs vary in different brain regions. The data show that STIM1 and STIM2 are present in the brain, thus both can be involved in CCE, depending on neuronal type.

Key words: capacitative calcium entry, CCE, STIM1, STIM2, neurons, brain, endoplasmic reticulum

INTRODUCTION

Multiple roles played by calcium ions as secondary messenger makes spatiotemporal properties of the calcium signals of the crucial importance. The frequency of synaptic calcium signals regulates the direction of plastic changes in the synapse; high frequency leads to long-term potentiation, while low frequency results in long-term depression (Tsumoto et al. 1996). Similarly, the localization of calcium entry site decides on its role. Calcium influx through NMDA receptor channel in extrasynaptic location is believed proapoptotic, while synaptic calcium is recognized as trophic signal (for review see Papadia and Hardingham 2007). Perturbations in calcium homeostasis are implicated in Alzheimers's disease (reviewed in Bojarski et al. 2008), and other neurodegenerative diseases, (reviewed in Wojda et al. 2008), as well as during ageing (reviewed in Puzianowska-Kuznicka and Kuznicki 2009).

Correspondence should be addressed to A. Skibinska-Kijek
Email: askib@iimcb.gov.pl

Received 12 October 2009, accepted 04 December 2009

Capacitative calcium entry (CCE) or store-operated calcium entry (SOCE) is considered to be an important element of calcium signaling and homeostasis in non-excitable cells (reviewed in Berridge et al. 2003). CCE is started when calcium stores in endoplasmic reticulum are emptied as a result of activation of IP3 and/or ryanodine receptors. Its role is to allow calcium influx through store operated calcium channels (SOC) and therefore provide calcium ions for replenishment of the stores. In neurons, this process was believed absent or negligible because of differences in magnitude between CCE and voltage-dependent calcium signals. The role of calcium source for calcium store refill was attributed to Na^+/Ca^{2+} exchanger (for review see Putney Jr. 2003).

However, growing number of reports shows that CCE is indeed present in neurons and that it plays an important role in neuronal physiology and survival. CCE was observed in hippocampal and cortical neurons in culture (Bouron at al. 2000, Prothero et al. 2000, Emptage et al. 2001, Baba et al. 2003) and it was shown to increase frequency of mIPSP (miniature inhibitory postsynaptic potentials) (Savic and Sciancalepore 1998) and mEPSP (miniature excitatory postsynaptic potentials) (Emptage et al. 2001) in those

neurons. CCE was also shown to regulate neuronal plasticity; pharmacological inhibition of SOC channels attenuates LTP at Schaffer collateral-CA1 synapses (Baba et al. 2003). Alternations of SOCE cause deregulation of Ca^{2+} homeostasis and may lead to pathologies of the nervous system. The best examples are Huntington's (Bezprozvanny and Hayden 2004) and Alzheimer's diseases, where abnormal SOCE in neurons was reported by several groups (reviewed by Bojarski et al. 2008). Nonetheless, molecular mechanisms of SOCE in neurons are still not known, and there is little information in the literature about the presence of proteins, which might be involved in SOCE in neuronal cells (reviewed in Dziadek and Johnstone 2007).

STIM1 (Stromal Interacting Molecule-1) is a novel regulator of SOCE (Liou et al. 2005, Roos et al. 2005). STIM1 is localized in the ER membrane where it serves as a Ca^{2+} sensor *via* an EF-hand Ca^{2+} binding site located in the lumen of the ER (Dziadek and Johnstone 2007). Upon Ca^{2+} store depletion STIM1 redistributes into punctuate structures, moves closer to the plasma membrane and activates SOC channels (Liou et al. 2005, Zhang et al. 2005). There is a large body of evidence showing that cooperation of STIM1 with the plasma membrane protein ORAI1 (CRACM1) is crucial for a proper functioning of SOCE (Soboloff et al. 2006a, Peinelt et al. 2006, Zhang et al. 2006, Liao et al. 2008). In mammalian cells, STIM1 has a close homolog, STIM2 (Williams et al. 2001, Soboloff et al. 2006b). Both proteins are similar with respect to their primary amino acid sequence, predicted secondary structure and domain organization. They diverge significantly within the C-terminal domain. STIM1 is expressed within the ER and at the cell surface, whereas STIM2 is expressed only in ER (Soboloff et al. 2006b, Dziadek and Johnstone 2007). We showed earlier that STIM1 is present in neurons and it undergoes intracellular translocation that is characteristic for CCE activation in non-excitable cells (Klejman et al. 2009). The depletion of the Ca^{2+} stores in cultured cortical neurons induced a change in the localization of YFP-STIM1 and ORAI1 from disperse, in untreated, to puncta-like in thapsigargin treated cells. We therefore proposed that in neurons, just as in non-excitable cells, the ORAI1 and STIM1 proteins are involved in store operated Ca^{2+} entry (Klejman et al. 2009). The aim of present work was to determine detailed description of STIM1 protein distribution in the brain of C57Bl6/J mouse and to compare its level to STIM2 to provide the basis of understanding the functions of both STIM proteins in neurons.

METHODS

All animals used in this study were cared for in accordance with the European Communities Council Directive (86/609/EEC). Experimental procedures were approved by the Local Commission for the Ethics of Animal Experimentation no. 1 in Warsaw.

Real Time PCR analysis

mRNA was purified from mouse brain structures using RNeasy Lipid Tissue Mini Kit (Qiagen). First-strand cDNA (prepared with SuperScript II, Invitrogen) was examined by quantitative Real Time PCR with specific gene primers for *Stim1* (5'GCTCTCAATGCCATGCCTTCCAAT, 5'TCTAGGCCATGGTTCAACGCCATA), *Stim2* (5'AGGGCAACTTGACACAGACAGGAT, 5'AGCAGTAGTTTATGCCGCTCTCGT), and SYBR Green dye (Applied Biosystems). The samples were analyzed using 7000 Sequence Detection System hardware and software (Applied Biosystems). 18S RNA for normalization was used with the following primers: 5'AACGAACGAGACTCTGGCATG, 5'CGGACATCTAAGGGCATCACA. Relative quantification (RQ) method was used to calculate relative levels of *Stim1* and *Stim2* mRNA, assuming equal efficiency of both PCR reactions. The formula was as follow: $RQ = 2^{-deltaCT}$, where deltaCT = CT(target) – CT(18S). The experiments were performed on adult FVB mice (8 weeks old).

Immunoblotting

Total protein extracts from mouse brain structures were prepared in RIPA buffer [50 mM Tris pH 7.5, 150 mM NaCl, 1% NP-40, 0.5% NaDOC, 0.1% SDS, 1 mM EDTA, protease inhibitors (Roche) and phosphatase inhibitors (Sigma)]. Brain tissue was homogenized on ice using glass-glass homogenizer (70 strokes) and cleared by centrifugation at 12 000 × g for 10 min. Protein extracts were separated on 8% SDS-PAGE gel and transferred to a Protran nitrocellulose membrane (Whatman). The membranes were immunostained with the appropriate antibodies. We used the following

rabbit polyclonal antibodies: STIM1 (ProteinTech Group Inc.), STIM2 (CT, ProSci Incorporated) and GAPDH (Santa Cruz). The intensity of the bands was measured using GS-800 Calibrated Densitometer and Quantity One software (Biorad). The experiments were performed on adult FVB mice (8 weeks old).

Immunohistochemistry

The experiments were performed on six C57Bl6/J adult (8 weeks) mice of both sexes. Mice were anesthetized with pentobarbitane and perfused transcardially, first with 50 ml of phosphate buffered saline (PBS, Sigma) and then with 50 ml of 4% formaldehyde in 0.1 M phosphate buffer, pH 7.4 (PB). The brains were removed, postfixed in fresh fixative for 3 days at 4°C and cryoprotected in 30% sucrose. The brains were then frozen in heptane and stored at –80°C. Sections of 40 μm were cut in cryostat, collected in PBS with 0.02% sodium azide as preservative and stored at 4°C until stained.

The endogenous peroxidase activity was quenched with 3% H_2O_2 in PBS. The sections were permeabilized with 0.1% Triton X-100 in PBS and blocked with 10% normal goat serum (NGS, Vector Laboratories) and 0.2% bovine serum albumin (BSA, histochemical grade, Sigma) in PBS containing 0.01% sodium azide overnight at 4ºC. Endogenous biotin was blocked using Avidin/Biotin Blocking Kit (Vector) according to manufacturer protocol.

The sections were incubated overnight at 4°C with antibody recognizing STIM1 (ProteinTech Group Inc., cat no 11565-1-AP, the antibody was raised against N-terminal fragment of the protein, aa 2-350) diluted 1:1 000 in PBS with 1% NGS, 0.2% BSA, 0.1% Triton and 0.01% sodium azide, washed and incubated with a biotinylated secondary antibody (Vector) in PBS containing 1% NGS, 0.2% BSA, 0.1% Triton and 0.01% sodium azide for 2 h at 4°C. After washing, the sections were incubated with Avidin-biotin complex reagent (ABC Elite kit, Vecor) according to the manufacturer protocol. The immunocomplex was visualized with DAB (Sigma).

Mounted sections were dehydrated in graded alcohol, mounted with DePeX (Serva). Omission control sections (without primary antibody) showed no specific immunostaining (not shown). Images were captured and analyzed using light microscope Nikon Eclipse 80i and Image-Pro Plus software. Brain regions were identified based on a Nissl-stained adjacent sections and "The Mouse Brain in Stereotaxic Coordinates" atlas by Paxinos and Franklin (2001). Brightness and contrast of images was adjusted with Adobe Photoshop CS4 Extended to ensure even background between captured sections. The immunostaining intensity was scored as follows: ++++, very strong; +++, strong; ++ moderate; + low.

The primary antibody specificity was confirmed by subjecting brain sections from STIM1 knockout mice to the procedure described above. Three 4 weeks old female STIM1-/- and three C57Bl6/J littermates were a kind gift by Prof. Benhardt Nieswandt, Rudolf Virchow Center, Würzburg, Germany. On sections from knockout animals only a residual staining was present in Purkinje and in molecular layers of the cerebellum. Staining pattern in wild-type animals did not differ from that presented here for older mice, though staining intensity seemed lower.

Double immunostaining

The experiments were performed on four mice of both sexes. Mice were anesthetized and perfused as described in Immunohistochemistry section. Brains were criosectioned to 20 μm sections. Sections were collected in PBS solution. Formaldehyde induced autofluorescence was quenched by incubation in 0.3M glycine solution in PBS. Next steps followed protocol described above in Immunohistochemistry section, only Streptavidin/Biotin Blocking Kit was used instead of Avidin/Biotin one. Both primary antibodies were incubated simultaneously and anti-NeuN antibody (Chemicon) was used at 1:1 000 dilution. Secondary antibodies were as follows: biotinylated goat anti-rabbit (Vector, 1:500) and Alexa Fluor488 conjugated goat anti-mouse (Invitrogen, 1:2 000). Biotinylated secondary antibody was detected using Alexa Fluor568 conjugated streptavidin (Invitrogen, 1:500). Sections were counterstained with Hoechst reagent. All appropriate controls for detection systems specificity and possible antibody cross-reactions were run and they showed no unspecific staining (not shown).

RESULTS

STIM1 and STIM2 expression in the mouse brain

We performed quantitative Real Time PCR to measure the level of *Stim1* and *Stim2* mRNA in various regions of the brain. RNA preparations obtained from

each brain structure of four to eight mice were analyzed independently. In all regions examined *Stim1* was expressed, although its level was lower than that of *Stim2*. About 7-fold difference was observed in hippocampus and 3-fold difference in cerebellum, thalamus, cortex and amygdala (Fig. 1A).

We next analyzed the level of STIM1 and STIM2 in total protein extracts from various structures of the mouse brain. Protein extracts prepared from three to four mouse brains were independently analyzed. The highest level of STIM2 was found in hippocampus with lower but similar levels in cerebellum, thalamus, cortex and amygdala (Fig. 1B). The densitometric analysis of the band intensities indicated that in hippocampus there was 5–10 times more STIM2 than in the other brain regions. STIM1 distribution pattern was identical to the one we described previously (Klejman et al. 2009). As previously, apart of approximately 90 kDa main band, we observed an additional double band for STIM1 immunoreactivity at 77 kDa in cerebellum.

Primary antibody characterization

The rabbit polyclonal anti-STIM1 antibody (ProteinTech Group Inc.) intended to use for immunohistochemistry was tested for specificity. First, to exclude possible STIM1 and STIM2 cross-reactivity, we transfected HEK cells (Human Embryonic Kidney cells) with YFP-tagged STIM constructs or with YFP. The antibody recognized YFP-STIM1 recombinant protein on Western-blot, but not YFP-STIM2 (not shown). Moreover, the pre-incubation of STIM1 antibody with the antigen peptide at 1:10 (approximated molar ratio), destroyed its ability to stain brain sections of wild type mice (Fig. 2C) as well as to recognize STIM1 band on the blots containing brain, HEK cells or lymphocytes protein extracts (not shown). The antibody did not stain brain sections from STIM1 knockout mice, except for a residual staining in Purkinje layer and molecular layer of the cerebellum, which are regions of the highest STIM1 immunoreactivity in wild type animals (Fig. 2).

STIM1 localization in the mouse brain

STIM1 immunoreactivity showed wide, but not uniform, distribution throughout the brain and it was observed in neuropil and in cells as cytoplasmic staining surrounding immunonegative nuclei. In hypothalamus and olfactory bulb high immunostaining was observed, moderate in the hippocampus, while low in most regions of the thalamus. Purkinje neurons and their dendrites showed the highest immunoreactivity. High immunoreactivity was also present in choroid plexus. Staining was absent in white matter nerve fibers, but cellular components were immunopositive there. Except for Purkinje neurons dendritic staining was rarely noted. In the barrel field region high level of staining in barrel hollows suggests immunoreactivity of axonal endings. Neither sexual dimorphism nor asymmetry between hemispheres was observed in the staining pattern or intensity. STIM1 protein distribution in various brain regions is summarized in Table I.

Telencephalon

In olfactory bulb, robust staining was present in mitral cells and in neuropil of external plexiform layer. Individual glomerules in glomerular layer were immunoreactive, but the signal intensity was lower. Moderate intensity signal was noted in granular cell layer of the olfactory bulb (Figs 3A, 7C). Within olfactory related regions, piriform cortex and olfactory tubercle showed strong staining (Fig. 3B). Tenia tecta, anterior olfactory nucleus and endopiriform nucleus were moderately stained. Within basal ganglia, caudate putamen was strongly stained and nucleus accumbens had strong signal (Fig. 3C). Globus pallidus had little staining. Within cerebral cortex, which in general was moderately stained, robust staining of a subset of layer V pyramidal neurons was observed (Fig. 7A). Layer related pattern was observed in the cortex. Supragranular layers were highly stained, and both cells and neuropil were immunoreactive. Granular layer had lowest signal, with the exception of barrel field region where intense staining was present in areas corresponding to the barrel hollows. Within infragranular layers, low neuropilar staining and strong pyramidal neurons immunoreactivity was observed in layer V, layer VI had moderate signal in cells and neuropil. Predominantly numerous immunoreactive pyramidal neurons were observed in retrosplenial cortex. Perirhinal cortex and ectorhinal cortex had strong signal. Septum was weakly stained. Within the hippocampus, an area of moderate signal, dentate gyrus was intensely stained in granular and molecular layers (Fig. 6A). CA1 and CA2 regions showed higher

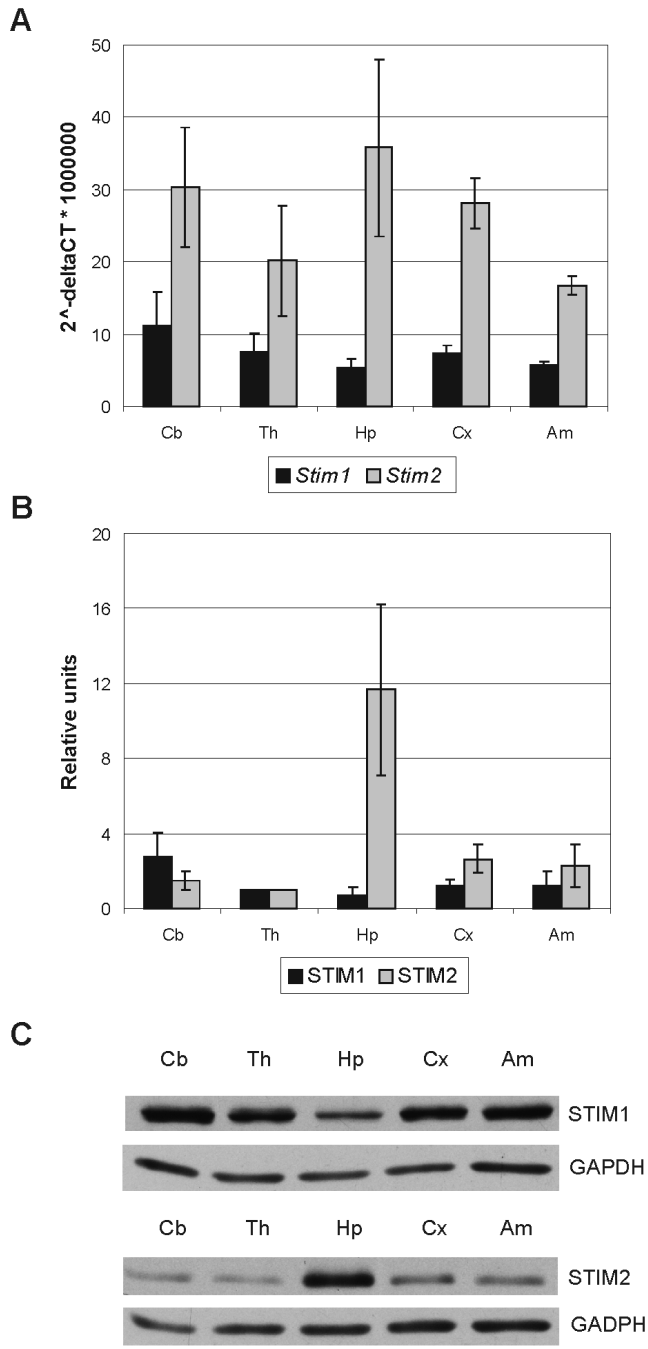

Fig. 1. Expression and distribution of STIM1 and STIM2 in the mouse brain. (A) the level of *Stim1* and *Stim2* mRNA in different mice brain regions. RNA was isolated from cerebellum, thalamus, hippocampus, cortex and amygdala. *Stim1* (black bars) and *Stim2* (grey bars) transcripts were detected by Real Time PCR with the specific probes. Values for *Stim1* or *Stim2* were normalized to 18S using RQ=$2^{-\text{deltaCT}}$ formula. The graph represents results obtained with four to eight mice. The error bars indicate SD. (B) Protein levels of STIM1 (black bars) and STIM2 (grey bars) in total protein extracts from cerebellum (Cb), thalamus (Th), hippocampus (Hp), cerebral cortex (Cx) and amygdala (Am) of the mouse brain were determined by Western Blot analysis. First, STIM1 or STIM2 bands, analyzed densitometrically, were normalized to the level of the loading control GAPDH for each immunoblot. Next, the signals from the thalamus were assigned an arbitrary number (1) and all other bands were expressed as a fraction of this value. Three to four mice were taken for independent immunoblottings. The error bars represent the SDs. (C) Representative immunoblot using STIM1 and STIM2 antibodies; for STIM1 only quantified band is shown.

immunoreactivity than CA3, and pyramidal cell layer was less intensively stained than neuropil layers. Amygdalo-hippocampal area was weakly stained. The profound differences in staining intensity were found in amygdala. Medial, basomedial, central amygdaloid nuclei and amygdalostriatal transition area were highly immunoreactive with both cells and neuropil staining. Cortical amygdaloid nuclei had slightly less signal and lateral and basolateral nuclei showed weak immunoreactivity (Fig. 6B).

Diencephalon

Hypothalamus showed very high immunoreactivity. Robust staining of cells and neuropil was observed in ventromedial (Fig. 7B) and arcuate hypothalamic nuclei (Fig. 3D). Paraventricular and anterior hypothalamic nuclei were moderately stained. Moderate immunoreactivity was observed in mammillary bodies. Preoptic area showed low to moderate staining. Within thalamus, little or no staining was observed with the exception of paraventricular thalamic nucleus which showed moderate immunoreactivity (Fig. 4A). Within posteromedial and posterolateral thalamic nuclei, numerous immunopositive cells were noted. Medial habenullar nucleus had moderate signal, and lateral habenullar nucleus was weakly stained (Fig. 4A).

Mesencephalon

Within midbrain, intensive staining was observed in superficial layers of the superior colliculi (Fig. 4B). Zonal layer and superficial gray layer showed very high neuropil staining and in optic nerve layer additionally highly immunoreactive cells were present. Deep layers of superior colliculi and inferior colliculi were weakly stained. Additionally, both parts of substantia nigra had strong signal. Medial pretectal nucleus had mild staining. Periaqueductal gray matter showed moderate staining with both cells and neuropil immunoreactive, furthermore dorsal and median raphe nuclei were moderately stained. Moderate staining was also observed in interpeduncular and oculomotor nuclei.

Rhombencephalon

Within hindbrain, weak or no immunoreactivity was observed with the exception of motor trigeminal nucleus and facial nucleus which were moderately stained, and locus coeruleus which showed strong immunoreactivity of cells and neuropil (Fig. 5A). In the cerebellum, Purkinje neurons were very highly immunoreactive. Their dendrites in molecular layer were clearly visible and very strongly stained (Fig. 5B). The Purkinje neurons showed the highest immunoreactivity in the mouse brain. Granular layer of the cerebellum was moderately stained. No staining was observed in deep cerebellar nuclei.

Identification of STIM1 positive cells as neurons

Immunoreactive cell profiles we observed had shape and size characteristic for neurons. Distinctive size and morphology of Purkinje neurons were apparent. To

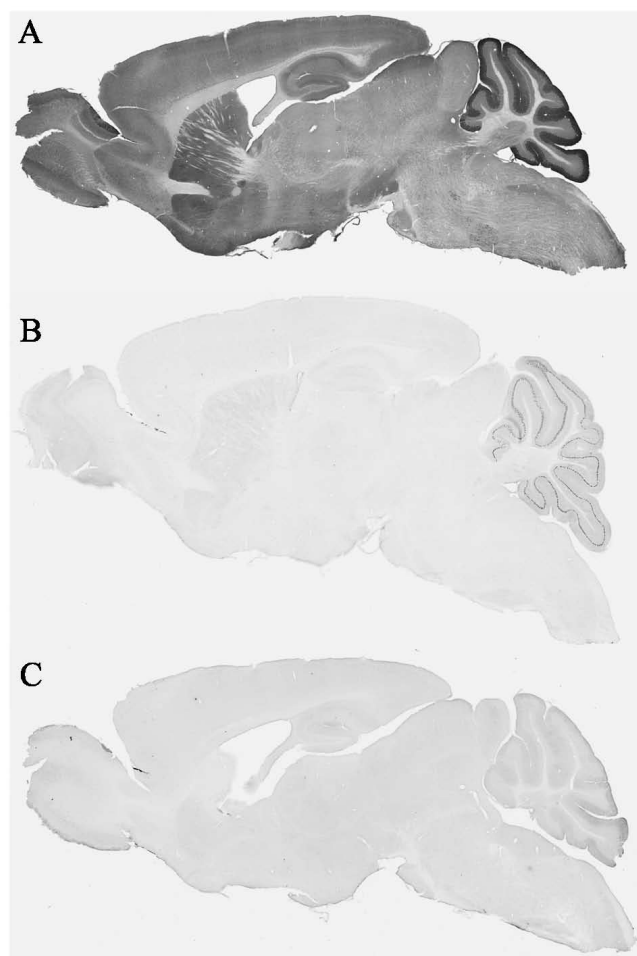

Fig. 2. Primary antibody characterization. (A) STIM1 immunoreactivity in the brain of C57Bl6/J mouse; (B) STIM1 immunoreactivity in the brain of STIM1 knockout mouse; (C) antibody pre-absorption control section from C57Bl6/J mouse.

Table I

STIM1 protein distribution in the adult mouse brain

Region	STIM1 immunoreactivity	Region	STIM1 immunoreactivity
Olfactory		Ectorhinal	++
Glomerular layer	++	Entorinal	+
External plexiform layer	+++	Basal ganglia	
Mitral cell layer	+++	Caudate/putamen	+++
Granular layer, olfactory	++	Nucleus accumbens	+++
Granular layer, accessory	++	Bed nucleus of the stria terminalis	++
Tenia tecta	++	Ventral pallidum	++
Piriform cortex	+++	Globus pallidus	+
Endopiriform nucleus	++	Amygdala	
Cortex		Central amygdaloid nucleus	+++
Cortical layer I	++	Basomedial amygdaloid nucleus	+++
Cortical layer II/III	+++	Basolateral amygdaloid nucleus	+
Cortical layer IV	+	Cortical amygdaloid nucleus	++
Cortical layer V	++	Medial amygdaloid nucleus	+++
Cortical layer VI	++	Lateral amygdaloid nucleus	+
Audiory	++	Amygdalohippocampal area	+
Sensory	++	Amygdalostriatal transition area	+++
Motor	+	Septum	
Cingulate	++	Septohippocampal nucleus	+
Orbital	++	Lateral septal nucleus	+
Visual	+	Hippocampus	
Retrosplenial	++	CA1	++
Perirhinal	++	CA2	++

Region	STIM1 immunoreactivity	Region	STIM1 immunoreactivity
CA3	+	Posterior hypothalamic area	+++
Pyramidal cell layer	+	Supramammillary	++
Stratum radiatum	+	Lateral mammillary	++
Stratum lacunosum moleculare	++	Preoptic area	
Stratum oriens	++	Medial preoptic area	++
Dentate gyrus molecular layer	++	Ventromedial preoptic nucleus	+
Dentate granular layer	++	Midbrain	
Dentate polymorph cell layer	+	Medial pretectal nucleus	+
Subiculum	++	Periaqueductal gray	++
Epithalamus		Substantia nigra	+++
Lateral habenular nucleus	+	Superior colliculus, zonal layer	+++
Medial habenular nucleus	++	Superior colliculus, superficial gray layer	+++
Thalamus		Superior colliculus, optic nerve layer	+++
Paraventricular thalamic nucleus	++	Dorsal raphe	++
Ventroposteromedial thalamic nucleus	+	Median raphe	++
Ventroposterolaterall thalamic nucleus	+	Interpeduncular nucleus	++
Hypothalamus		Oculomotor nucleus	++
Paraventricular nucleus	++	Motor trigeminal nucleus	++
Anterior nucleus	++	Facial nucleus	++
Ventromedial nucleus		Locus coreuleus	+++
Dorsomedial part	+++	Cerebellum	
Ventrolateral part	++	Purkinje cells	++++
Arcuate nucleus	+++	Granular cell layer	++

present the final prove that STIM1 indeed is present in neurons in other brain regions, we performed double staining with neuronal marker ccccccial amygdaloid nucleus (B), basolateral amygdaloid nucleus (C), ventromedial hypothalamic nucleus (D). Thus, we demonstrate neuronal localization of STIM1 in these brain regions.

DISCUSSION

In the present work we provide detailed description of STIM1 distribution in the mouse brain. First, we show that STIM1 mRNA and protein can be detected in extracts of all major parts of the brain. This is a in good agreement with Williams and coworkers (2001), who showed that the mRNAs encoding both *Stim1* and *Stim2* are expressed in human brain samples.

Second, we found by real time PCR that in hippocampus there is about 7-fold lower amount of *Stim1* mRNA as compared to *Stim2*, but in other brain regions only 3-fold lower. This is in agreement with data presented by Berna-Erro and others (2009), who also observed more STIM2 than STIM1 in the brain. However, these authors claim that their immunocytochemical analysis revealed hardly any immunosignal for STIM1 in cultured hippocampal neurons. Moreover, based on the lack of *Stim1* message in RNA samples obtained from isolated neurons and analyzed by

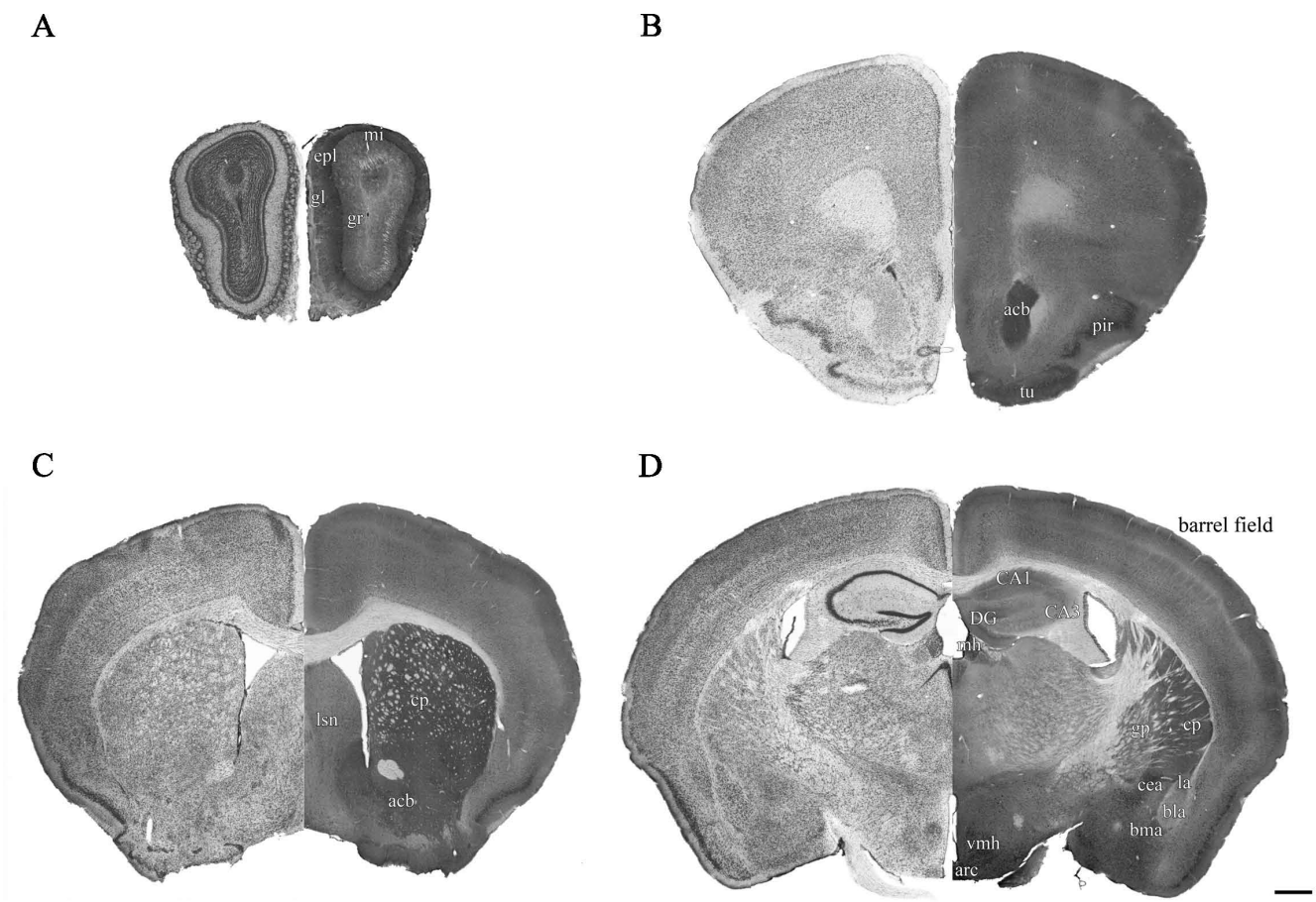

Fig. 3. Immunohistochemical localization of STIM1 in the mouse brain. STIM1 IHC sections are presented on the right side of each panel, left sides of the sections were replaced with Nissl stained adjacent sections. (mi) mitral cell layer; (epl) external plexiform layer; (gl) glomerular layer; (gr) granular cell layer; (acb) nucleus accumbens; (pir) piriform cortex; (tu) olfactory tubercle; (lsn) lateral septal nucleus; (cp) caudate putamen; (CA1-3) fields of hippocampus; (DG) dentate gyrus; (mh) medial habenullar nucleus; (gp) globus pallidus; (vmh) ventromedial hypothalamic nucleus; (arc) arcuate hypothalamic nucleus; (la) lateral amygdaloid nucleus; (bla) basolateral amygdaloid nucleus; (cea) central amygdaloid nucleus; (bma) basomedial amygdaloid nucleus. Scale bar is 500 μm.

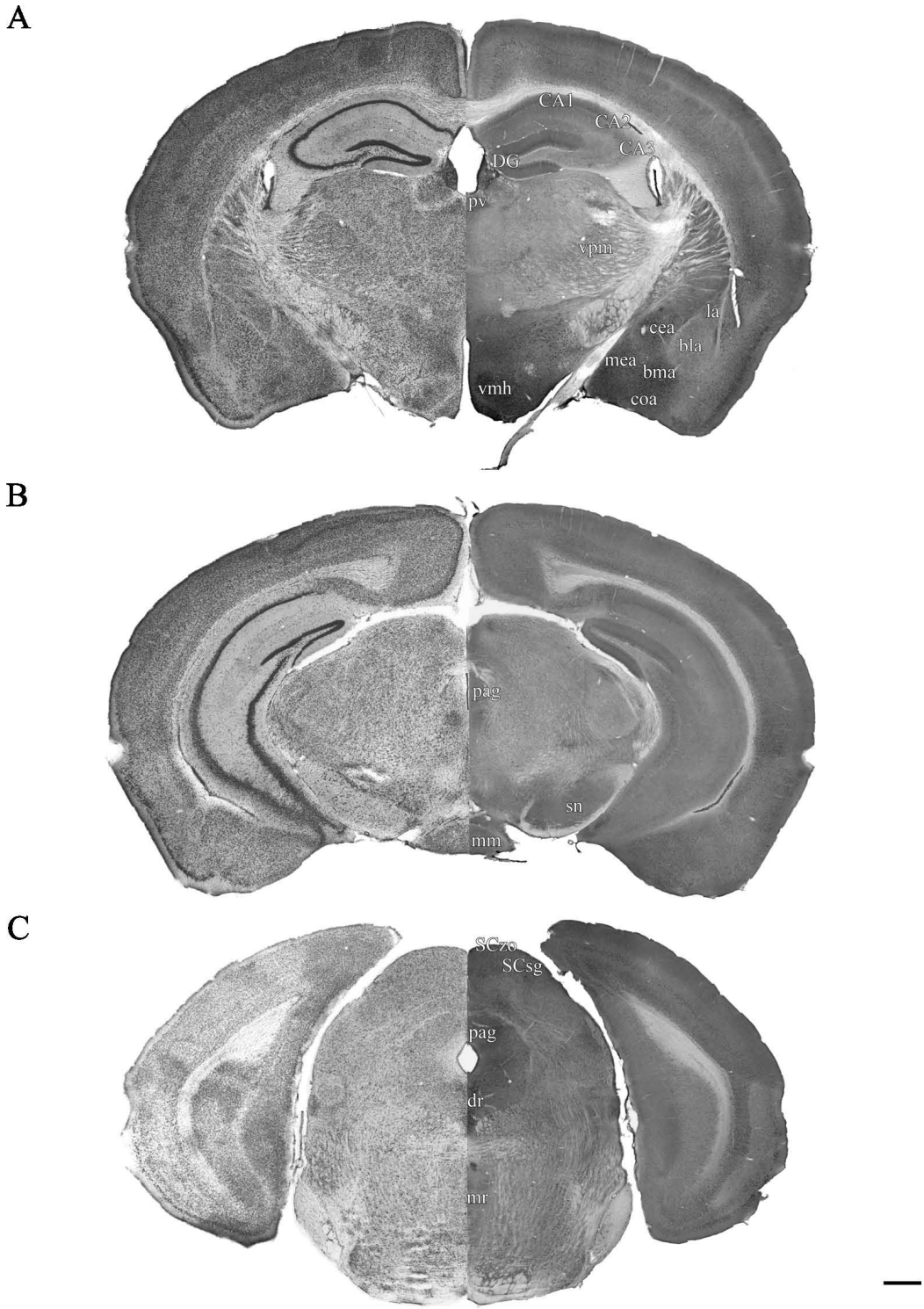

Fig. 4. Immunohistochemical localization of STIM1 in the mouse brain. STIM1 IHC sections are presented on the right side of each panel, left sides of the sections were replaced with Nissl stained adjacent sections. (CA1-3) fields of hippocampus; (DG) dentate gyrus; (vmh) ventromedial hypothalamic nucleus; (la) lateral amygdaloid nucleus; (bla) basolateral amygdaloid nucleus; (cea) central amygdaloid nucleus; (coa) cortical amygdaloid nucleus; (mea) medial amygdaloid nucleus; (bma) basomedial amygdaloid nucleus; (vpm) ventral posteromedial thalamic nucleus; (pv) paraventricular thalamic nucleus; (pag) periaqueductal gray matter; (sn) substantia nigra; (mm) mammillary bodies; (SCzo) superior colliculus zonal layer; (SCsg) superior colliculus superficial gray layer; (dr) dorsal raphe; (mr) median raphe. Scale bar is 500 μm.

reverse transcription PCR, they suggest that STIM1 signals derive from cells other than neurons. This is in contrast to our published data (Klejman et al. 2009), which indicate that STIM1 can be detected, and co-localized with ER marker calreticulin, not only in hippocampal neurons, but also in cortical neurons *in vitro*. The reason for this discrepancy is not clear.

Third, we identify specific regions in the mice brain which have high, medium and low STIM1 immunoreactivity and using co-immunostaining with NeuN we prove that STIM1 positive cells are neurons. We think that the immunoreactivity pattern of STIM1 presented in this work is specific, i.e. resembling the authentic protein distribution *in situ* for two major reasons. The specificity of the STIM1 antibody we used cannot be questioned because it did not stain brain sections from STIM1 knockout mice. The residual staining in the Purkinje and molecular layer of the cerebellum, the regions of the highest STIM1 immunoreactivity in wild type animals, can be explained by the likely "leaky" knockout technique used to create these mice. The STIM1-/- mice were generated by means of gene disruption technique, which should result with expression of a fusion protein consisting of N-terminal fragment of STIM1 and β-galactosidase (Varga-Szabo et al. 2008). STIM1-β-galactosidase fusion protein should be rapidly degraded and indeed it was not detected on Western-blots (Varga-Szabo et al. 2008). However, this fusion protein contains epitope recognized by the antibody used in our experiments, and residual even partly cleaved STIM1 could be detected in the regions of the highest STIM1 content in STIM1-/- knockout mice.

The specificity of immunostaining can be also proved by the fact that the preincubation of STIM1 antibody with the antigen peptide which was used for immunization, destroyed its ability to stain brain sections of wild type mice as well as to recognize STIM1 band on the blots containing brain or lymphocytes protein extracts.

We detected very high STIM1 immunosignal in Purkinje cells and their dendrites. This suggests an important role of STIM1 in calcium homeostasis in Purkinje neurons, especially in light of immunoblotting data showing low level of STIM2 in the cerebellum. High level of STIM1 protein was observed in hypothalamus, caudate putamen and nucleus accumbens and in other regions providing neuromodulatory input: substantia nigra, dorsal raphe and locus coeruleus. Robust level of STIM1 protein is present in olfactory related regions and in the cortico-medial region of the amygdala, associated with the olfactory system. In contrast, evolutionarily newer division of the amygdala, basolateral region has low STIM1 protein level. Basolateral amygdala is associated with neocortex, which has moderate level of STIM1 protein. Other cortical regions and hippocampus show similar to each other STIM1 immunosignal, which are stronger than those observed in basolateral amygdala. Although, in

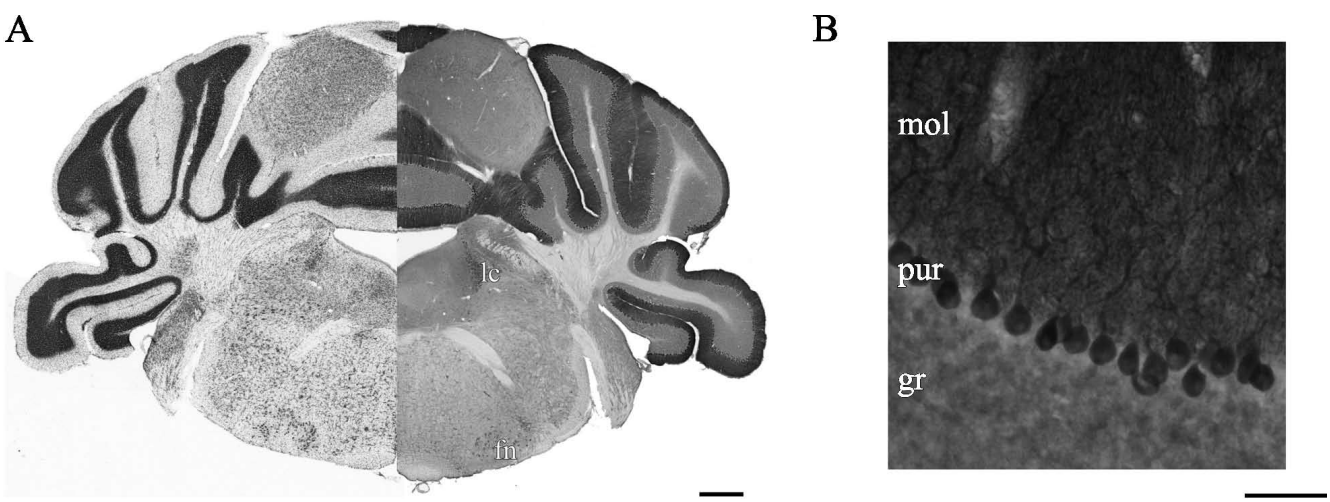

Fig. 5. Immunohistochemical localization of STIM1 in the mouse brain. (A) STIM1 IHC section is presented on the right side of a panel, left side of the section was replaced with Nissl stained adjacent section. (lc) Locus coeruleus; (fn) facial nucleus. Scale bar is 500 μm. (B) Higher magnification of STIM1 immunostained cerebellar cortex. (mol) Molecular layer; (pur) Purkinje cells layer; (gr) granular cells layer. Scale bar is 100 μm.

cerebral cortex immunoreactive neurons could be distinguished counter to neuropil staining, in the hippocampus neuropil staining was higher than the staining observed in the pyramidal cell bodies.

Analysis of STIM1 and STIM2 regional distribution on protein and mRNA level shows that STIM2 predominates in the hippocampus but in cerebellum the levels of STIM1 and STIM2 are similar. The

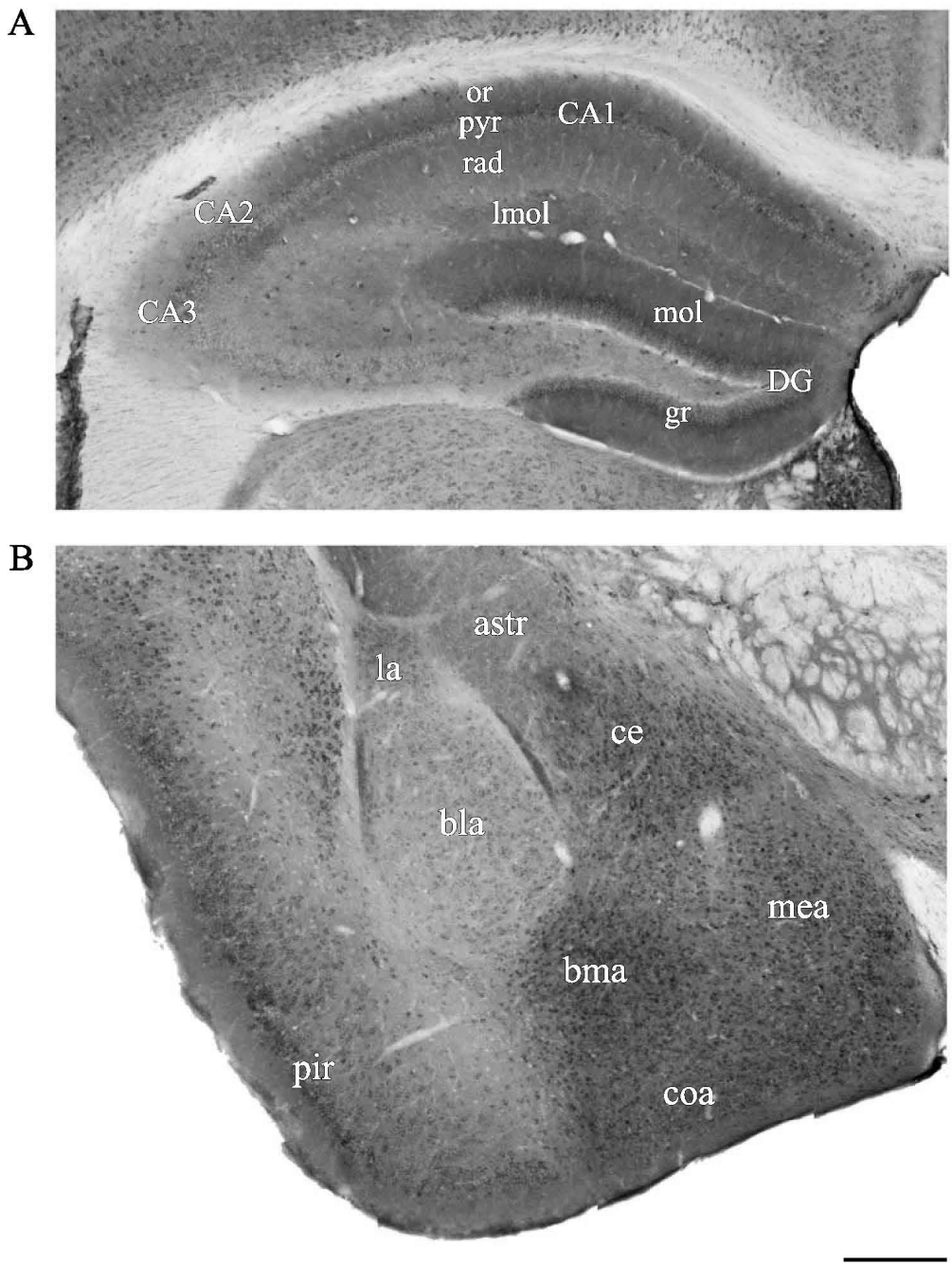

Fig. 6. Immunohistochemical localization of STIM1 in the mouse brain. (A) higher magnification of the hippocampus. (CA1-3) fields of hippocampus; (DG) dentate gyrus; (or) stratum oriens; (pyr) stratum pyramidale; (rad) stratum radiatum; (lmol) stratum lacunosum moleculare; (mol) molecular layer; (gr) granular layer. (B) higher magnification of the amygdala. (la) lateral amygdaloid nucleus; (bla) basolateral amygdaloid nucleus; (cea) central amygdaloid nucleus; (coa) cortical amygdaloid nucleus; (mea) medial amygdaloid nucleus; (astr) amygdalostriatal transition area. Scale bar is 300 μm.

other conclusion coming from these experiments is that STIM1 protein level follows mRNA expression profile, suggesting transcription mechanism as major control for protein level. In contrast, STIM2 protein level does not seem to depend strictly on mRNA level, pointing to more complex regulation of STIM2 protein level. This suggests that results by Berna-Erro and colleagues (2009) can be explained at least partly by the compensatory effects: STIM2 being more prone to expression regulation might compensate for STIM1 knockout, while STIM1 might not. We showed earlier that presenilin regulates the level of STIM2. In human lymphocytes with familial Alzheimer's disease presenilin mutations the level of STIM2 was decreased, while the level of STIM1 was unchanged. We also observed CCE attenuation in those cells. Thus, it is the ratio between these two ER calcium sensors

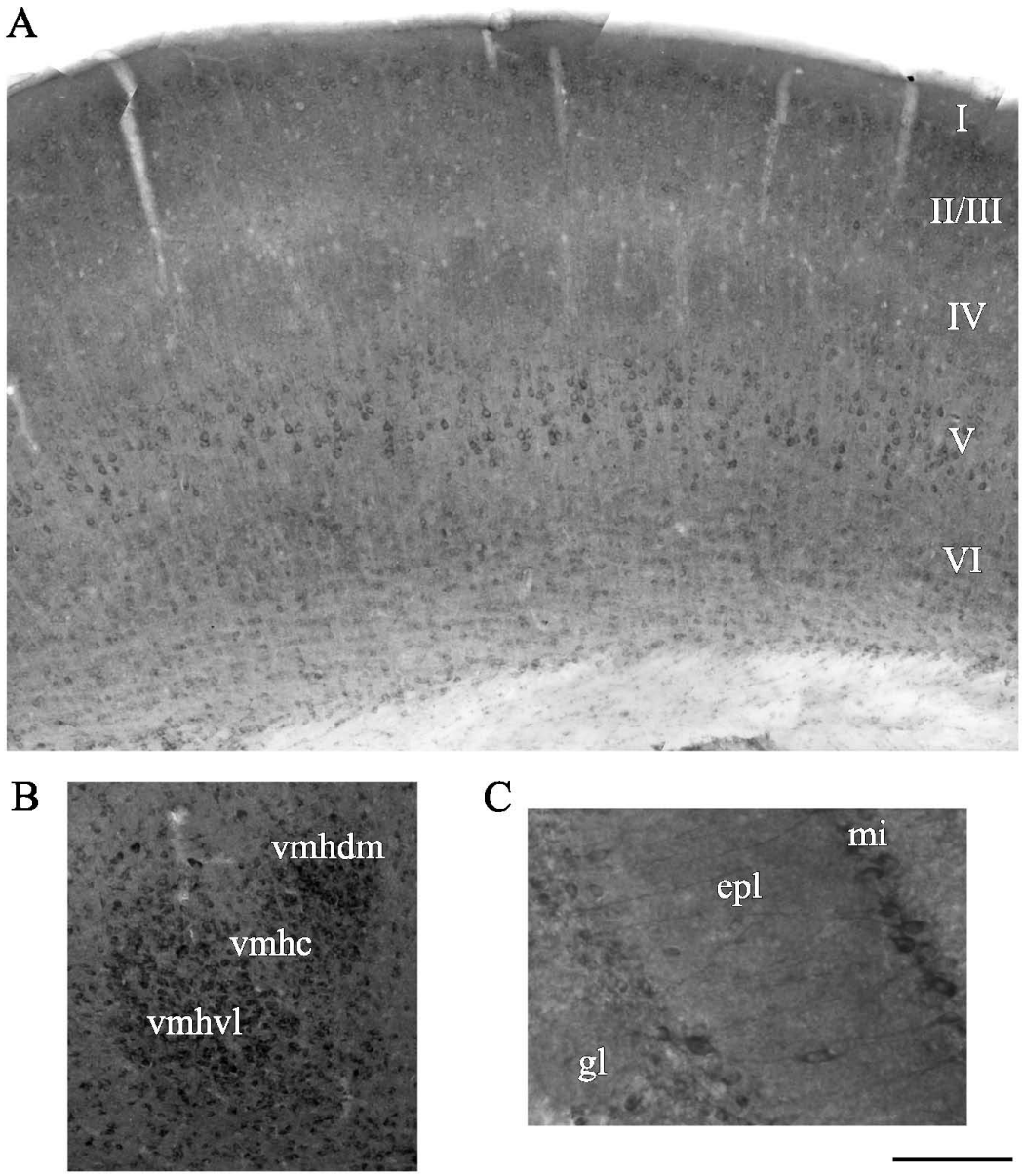

Fig. 7. Immunohistochemical localization of STIM1 in the mouse brain. (A) higher magnification of the primary somatosensory cortex, barrel field region. (B) higher magnification of ventromedial hypothalamus. (vmhc) ventromedial hypothalamic nucleus central part; (vmhdm) ventromedial hypothalamic nucleus dorsomedial part; (vmhvl) ventromedial hypothalamic nucleus ventrolateral part. Scale bar is 200 μm. (C) higher magnification of olfactory bulb. (mi) Mitral cells layer; (epl) external plexiform layer; (gl) glomerular layer. Scale bar is 100 μm.

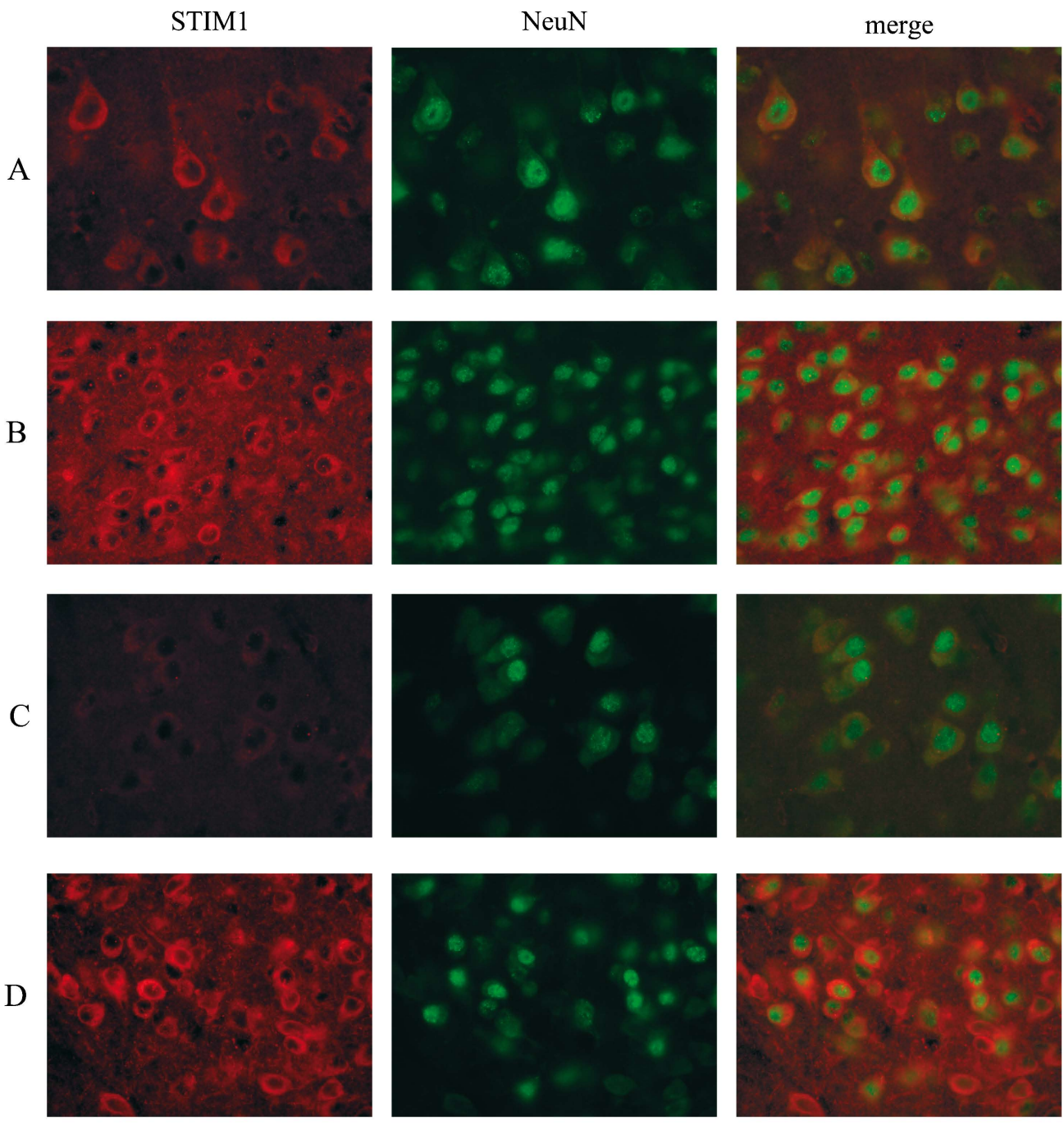

Fig. 8. Identification of STIM1 immunopositive cells as neurons in (A) primary somatosensory cortex layer V, (B) medial amygdaloid nucleus, (C) basolateral amygdaloid nucleus, (D) ventromedial hypothalamic nucleus. Note high STIM1 immunostaining of neuropil in medial amygdaloid nucleus and in ventromedial hypothalamic nucleus.

which seems to determine the CCE profile (Bojarski et al. 2009).

We showed earlier that depletion of the Ca^{2+} store in cultured cortical neurons induces a change in the localization of YFP-STIM1 and ORAI1 from disperse, in untreated, to puncta-like in thapsigargin treated cells (Klejman et al. 2009). Thus, in neurons, just as in non-excitable cells, STIM1 protein can be involved in store operated Ca^{2+} entry created by proteins expressed from transfected plasmids.

CONCLUSION

We provide evidence for neuronal expression of STIM1 in the mouse brain. High level of this protein in certain brain regions indicate it plays a role in calcium homeostasis, likely in CCE. The data showing a different distribution of STIM1 and STIM2 in the mouse brain supports the idea that these two proteins have distinct modes of action in the brain, but do not seem to support the conclusion that only STIM2 is essential.

ACKNOWLEDGMENTS

This work was supported by the Polish-German grant to JK no. S001/P-N/2007/01 from the Polish Ministry of Science and Higher Education and to Dr. Jochen Herms no. 01GZ0713 from the Bundesministerium für Bildung und Forschung and by EU FPVI Promemoria Grant contract no. 512012. JK receives professorial fellowship from Foundation for Polish Science. We thank Dr. Atilla Braun and Professor Benhardt Nieswandt (Rudolf Virchow Center DFG Research Center for Experimental Biomedicine, and Institute of Clinical Biochemistry and Pathobiochemistry, University of Würzburg, Würzburg, Germany) for brains of STIM1 knockout mice. We thank Dr. Monika Klejman and Dr. Wojciech Michowski for their help in some experiments.

REFERENCES

Baba A, Yasui T, Fujisawa S, Yamada RX, Yamada MK, Nishiyama N, Matsuki N, Ikegaya Y (2003) Activity-evoked capacitative Ca2+ entry: implications in synaptic plasticity. J Neurosci 23: 7737–7741.

Berna-Erro A, Braun A, Kraft R, Kleinschnitz C, Schuhmann MK, Stegner D, Wultsch T, Eilers J, Meuth SG, Stoll G, Nieswandt B (2009) STIM2 regulates capacitive Ca2+ entry in neurons and plays a key role in hypoxic neuronal cell death. Sci Signal 2: ra67.

Berridge MJ, Bootman MD, Roderick HL (2003) Calcium signalling: dynamics, homeostasis and remodelling. Nat Rev Mol Cell Biol 4: 517–529.

Bezprozvanny I, Hayden MR (2004) Deranged neuronal calcium signaling and Huntington disease. Biochem Biophys Res Commun 322: 1310–1317.

Bojarski L, Herms J, Kuznicki J (2008) Calcium dysregulation in Alzheimer's disease. Neurochem Int 52: 621–633.

Bojarski L, Pomorski P, Szybinska A, Drab M, Skibinska-Kijek A, Gruszczynska-Biegala J, Kuznicki J (2009) Presenilin-dependent expression of STIM proteins and dysregulation of capacitative Ca2+ entry in familial Alzheimer's disease. Biochim Biophys Acta 1793: 1050–1057.

Bouron A (2000) Activation of a capacitative Ca(2+) entry pathway by store depletion in cultured hippocampal neurones. FEBS Lett 470: 269–272.

Dziadek MA, Johnstone LS (2007) Biochemical properties and cellular localisation of STIM proteins. Cell Calcium 42: 123–132.

Emptage NJ, Reid CA, Fine A (2001) Calcium stores in hippocampal synaptic boutons mediate short-term plasticity, store-operated Ca2+ entry, and spontaneous transmitter release. Neuron 29: 197–208.

Klejman ME, Gruszczynska-Biegala J, Skibinska-Kijek A, Wisniewska MB, Misztal K, Blazejczyk M, Bojarski L, Kuznicki J (2009) Expression of STIM1 in brain and puncta-like co-localization of STIM1 and ORAI1 upon depletion of Ca(2+) store in neurons. Neurochem Int 54: 49–55.

Liao Y, Erxleben C, Abramowitz J, Flockerzi V, Zhu MX, Armstrong DL, Birnbaumer L (2008) Functional interactions among Orai1, TRPCs, and STIM1 suggest a STIM-regulated heteromeric Orai/TRPC model for SOCE/Icrac channels. Proc Natl Acad Sci U S A 105: 2895–900.

Liou J, Kim ML, Heo WD, Jones JT, Myers JW, Ferrell JE Jr, Meyer T (2005) STIM is a Ca2+ sensor essential for Ca2+-store-depletion-triggered Ca2+ influx. Curr Biol 15: 1235–1241.

Papadia S, Hardingham GE (2007) The dichotomy of NMDA receptor signaling. Neuroscientist 13: 572–579.

Paxinos G, Franklin KBJ (2001) The Mouse Brain in Stereotaxic Coordinates. Academic Press, San Diego, CA.

Peinelt C, Vig M, Koomoa DL, Beck A, Nadler MJ, Koblan-Huberson M, Lis A, Fleig A, Penner R, Kinet JP (2006) Amplification of CRAC current by STIM1 and CRACM1(Orai1). Nat Cell Biol 8: 771–773.

Prothero LS, Mathie A, Richards CD (2000) Purinergic and muscarinic receptor activation activates a common calcium entry pathway in rat neocortical neurons and glial cells. Neuropharmacology 39: 1768–1778.

Putney JW Jr (2003) Capacitative calcium entry in the nervous system. Cell Calcium 34: 339–344.

Puzianowska-Kuznicka M, Kuznicki J (2009) The ER and ageing II: calcium homeostasis. Ageing Res Rev 8: 160–172.

Roos J, DiGregorio PJ, Yeromin AV, Ohlsen K, Lioudyno M, Zhang S, Safrina O, Kozak JA, Wagner SL, Cahalan MD, Veliçelebi G, Stauderman KA (2005) STIM1, an essential

and conserved component of store-operated Ca2+ channel function. J Cell Biol 169: 435–445.

Savić N, Sciancalepore M (1998) Intracellular calcium stores modulate miniature GABA-mediated synaptic currents in neonatal rat hippocampal neurons. Eur J Neurosci 10: 3379–3386.

Soboloff J, Spassova MA, Tang XD, Hewavitharana T, Xu W, Gill DL (2006a) Orai1 and STIM reconstitute store-operated calcium channel function. J Biol Chem 281: 20661–20665.

Soboloff J, Spassova MA, Hewavitharana T, He LP, Xu W, Johnstone LS, Dziadek MA, Gill DL (2006b) STIM2 is an inhibitor of STIM1-mediated store-operated Ca2+ Entry. Curr Biol 16: 1465–1470.

Tsumoto T, Yasuda H, Fukuda M, Akaneya Y (1996) Postsynaptic calcium and calcium-dependent processes in synaptic plasticity in the developing visual cortex. J Physiol Paris 90: 151–156.

Varga-Szabo D, Braun A, Kleinschnitz C, Bender M, Pleines I, Pham M, Renné T, Stoll G, Nieswandt B (2008) The calcium sensor STIM1 is an essential mediator of arterial thrombosis and ischemic brain infarction. J Exp Med 205: 1583–1591.

Williams RT, Manji SS, Parker NJ, Hancock MS, Van Stekelenburg L, Eid JP, Senior PV, Kazenwadel JS, Shandala T, Saint R, Smith PJ, Dziadek MA (2001) Identification and characterization of the STIM (stromal interaction molecule) gene family: coding for a novel class of transmembrane proteins. Biochem J 357: 673–685.

Wojda U, Salinska E, Kuznicki J (2008) Calcium ions in neuronal degeneration. IUBMB Life 60: 575–590.

Zhang SL, Yu Y, Roos J, Kozak JA, Deerinck TJ, Ellisman MH, Stauderman KA, Cahalan MD (2005) STIM1 is a Ca2+ sensor that activates CRAC channels and migrates from the Ca2+ store to the plasma membrane. Nature 437: 902–905.

Zhang SL, Yeromin AV, Zhang XH, Yu Y, Safrina O, Penna A, Roos J, Stauderman KA, Cahalan MD (2006) Genome-wide RNAi screen of Ca(2+) influx identifies genes that regulate Ca(2+) release-activated Ca(2+) channel activity. Proc Natl Acad Sci U S A 103: 9357–9362.